



Pergamon

SCIENCE @ DIRECT®

Tetrahedron Letters 44 (2003) 4167–4169

TETRAHEDRON  
LETTERS

# Building molecular-scale bridges having restricted rotation

Andrew C. Benniston,\* Anthony Harriman, Peiyi Li and Craig A. Sams

*Molecular Photonics Laboratory, Bedson Building, School of Natural Sciences (Chemistry), University of Newcastle, Newcastle-upon-Tyne NE1 7RU, UK*

Received 20 March 2003; accepted 10 April 2003

**Abstract**—The synthesis is reported of a binuclear ruthenium(II) bis(2,2':6',2''-terpyridine) complex for which the polytopic ligand incorporates a central, torsionally-constrained biphenylene group. In principle, the dihedral angle between the two phenylene rings can be controlled by the length of the constraining strap. © 2003 Elsevier Science Ltd. All rights reserved.

Among the materials that could be used as molecular-scale wires, poly(phenylenes) look to be particularly promising candidates since they are known to conduct electronic charge over reasonably long distances. A major limitation of poly(phenylenes), however, is that internal rotation around the connecting C–C bond is facile. This leads to a multitude of conformers when the compound is dispersed in a solid medium. The reason why this heterogeneity is undesirable stems from the realisation that the rate of through-bond electron transfer depends on the mutual orientation of adjacent phenylene rings and can vary significantly with torsion angle. The maximum rate of information transfer along a poly(phenylene) wire most likely corresponds to the case where the phenylene rings are coplanar (Fig. 1).<sup>1</sup>

In attempting to optimise the rate of through-bond electron transfer in molecular-scale photoactive devices it seems prudent to attempt to control the mutual orientation of adjacent subunits that form the connecting wire. This is not an easy task but we describe herein a strategy for the design of new biphenylene linkers possessing constrained geometry. Our approach involves the synthesis of a biphenylene unit equipped with a short strap attached at the 2,2'-positions. This strap restricts rotation around the connecting C–C

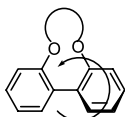
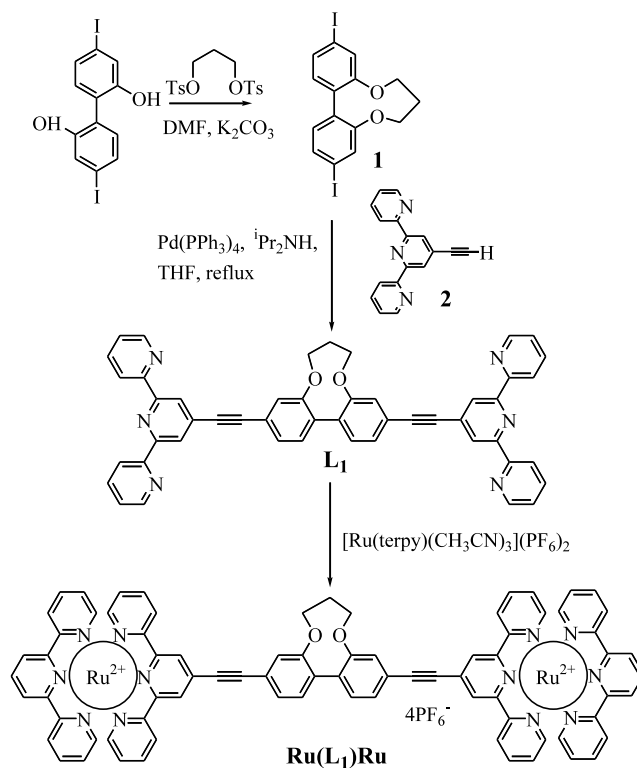


**Figure 1.** Restricted rotation in a constrained biphenyl unit.

\* Corresponding author. Tel.: +44-(0)191-222-5706; fax: +44-(0)191-222-6929; e-mail: [a.c.benniston@ncl.ac.uk](mailto:a.c.benniston@ncl.ac.uk)



**Scheme 1.** Synthetic procedure used for the preparation of **L<sub>1</sub>** and **[Ru(L<sub>1</sub>)Ru](PF<sub>6</sub>)<sub>4</sub>**.

bond whilst the electronegative O atoms prevent the phenylene rings adopting a coplanar orientation. The overall effect is to restrict the geometry. In principle, predetermined torsion angles between the phenylene rings could be realised by varying the length, and/or composition, of the strap.

In order to test this hypothesis, we have designed a novel binuclear ruthenium(II) bis(2,2':6',2''-terpyridine)-based molecular dyad having a central biphenylene connector (Scheme 1). The presence of the light-active terminals should allow proper evaluation of how the torsion angle affects the degree of electronic communication along the molecular axis. A small refinement in the design protocol requires the introduction of an alkynylene substituent placed at the 4'-position of the 2,2':6',2''-terpyridine ligand so as to improve the photo-physical properties of the corresponding ruthenium(II) complex. Hence, our primary target has been a binuclear ruthenium(II) bis(2,2':6',2''-terpyridine) complex built around a linear 4,4'-diethynyl biphenylene unit, which is itself strapped at the 2,2'-positions.<sup>2</sup>

Illustrated in Scheme 1 is the synthetic protocol used for construction of the ditopic ligand **L**<sub>1</sub> and its corresponding binuclear ruthenium(II) complex. Thus, 4,4'-diiodobiphenyl-2,2'-diol was prepared by literature methods,<sup>3</sup> starting from 3-nitroanisole and making use of the benzidine rearrangement reaction. The analogous strapped derivative **1** was prepared in good yield (56%) by reaction of 4,4'-diiodobiphenyl-2,2'-diol with 1,3-ditosyloxypropane.<sup>4</sup> Using standard Sonogashira cross-coupling conditions,<sup>5</sup> 4'-ethynyl-[2,2':6',2''-terpyridine] **2**<sup>6</sup> was attached to **1** so as to afford the ditopic ligand **L**<sub>1</sub> in 56% yield.<sup>7</sup> The ligand was purified by column chromatography on basic alumina with CH<sub>2</sub>Cl<sub>2</sub> as eluent. The corresponding binuclear complex Ru(**L**<sub>1</sub>)Ru was prepared by refluxing **L**<sub>1</sub> with a slight excess of [Ru(terpy)(CH<sub>3</sub>CN)<sub>3</sub>](PF<sub>6</sub>)<sub>2</sub><sup>8</sup> in a mixture of CHCl<sub>3</sub>/MeOH/CH<sub>3</sub>COCH<sub>3</sub>. The crude reaction product was purified by extensive column chromatography [basic alumina, CH<sub>3</sub>CN/H<sub>2</sub>O] and anion exchange with KPF<sub>6</sub>.<sup>9</sup> The complex gave satisfactory analysis when subjected to the usual analytical techniques.

In addition to the expected aromatic protons, the <sup>1</sup>H NMR spectrum of Ru(**L**<sub>1</sub>)Ru in *d*<sub>6</sub>-acetone revealed that the O-CH<sub>2</sub> protons of the propylene strap are fluxional. At room temperature, the signal corresponding to the four protons of the two O-CH<sub>2</sub> groups was broad and showed no obvious sign of a coupling pattern. Upon cooling the sample to -50°C, two clear signals emerged at ~4.56 and 4.59 ppm. These signals displayed obvious signs of coupling, which could be

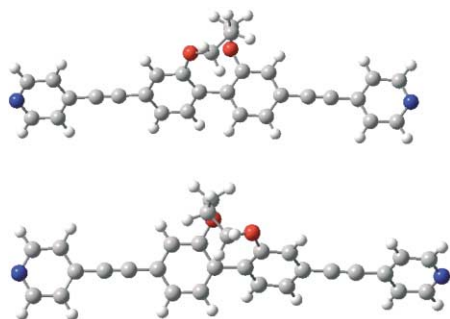


**Figure 2.** Computer generated ball and stick representations of the two conformations predicted for a simplified version of **L**<sub>1</sub>.

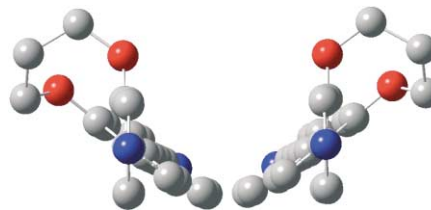


**Figure 3.** View along the axis of the two atropisomers of the **L**<sub>1</sub> analogue.

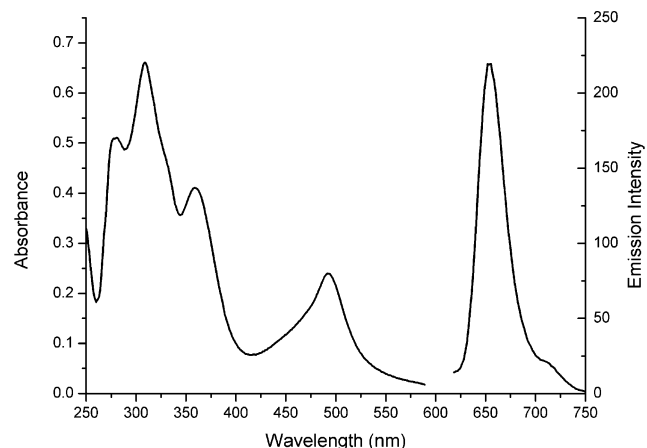


**Figure 4.** Absorption and emission profiles of Ru(**L**<sub>1</sub>)Ru recorded in butyronitrile. Note: emission spectrum was recorded at 77 K.

approximated to an AA'BB' pattern. The process by which the OCH<sub>2</sub> protons become inequivalent was assumed to involve restricted rotation around the connector carbon atoms of the biphenyl group.

Further insight into the molecular structure was sought using geometry optimisations performed using the Hartree–Fock method<sup>10</sup> in a CH<sub>3</sub>CN solvent bath for a version of **L**<sub>1</sub> that lacked the extra pyridine rings at the two terminals (Fig. 2). This molecule shows axial chirality due to restricted rotation around the biphenylene group (Fig. 3). In each atropisomer, the calculated dihedral angle for the biphenylene unit is ca. 51°. It is important to note, however, that there is considerable flexibility within this molecule. This is apparent from molecular dynamics simulations that report on the total variation in the torsion angle, which was found to be ±35°. Even so, the structure spends the vast majority of its lifetime with a torsion angle of 51±5°.

The terminal metal complexes present in Ru(**L**<sub>1</sub>)Ru show the anticipated metal-to-ligand charge-transfer (MLCT) absorption band around 500 nm (Fig. 4). It is clear that the presence of the constraining strap does not perturb the absorption spectrum. Weak phosphorescence can be detected for Ru(**L**<sub>1</sub>)Ru in butyronitrile at room temperature but the yield is greatly enhanced upon cooling to 77 K (Fig. 4). Under such conditions, the emission maximum lies at 655 nm and is red shifted by 50 nm with respect to that found for the parent

complex  $[\text{Ru}(\text{terpy})_2]^{2+}$ . This is because the total reorganisation energy accompanying deactivation of triplet  $\text{Ru}(\text{L}_1)\text{Ru}$ ,  $\lambda_T = 1030 \text{ cm}^{-1}$ , significantly exceeds that of the parent,  $\lambda_T = 510 \text{ cm}^{-1}$  due to extensive electron delocalisation in the former system. For both compounds, spectral curve fitting indicates that a Ru–N stretching vibration ( $\nu \approx 450 \text{ cm}^{-1}$ ) is coupled to deactivation of the triplet state, in addition to a higher frequency vibrational mode. This latter vibration differs markedly between  $\text{Ru}(\text{L}_1)\text{Ru}$  ( $\nu \approx 880 \text{ cm}^{-1}$ ) and the parent complex ( $\nu \approx 1380 \text{ cm}^{-1}$ ). Because of the presence of the alkyne substituent, it is most likely that the lowest-energy triplet state associated with  $\text{Ru}(\text{L}_1)\text{Ru}$  is formed by charge injection from the metal centre to the substituted terpyridine ligand. The enlarged reorganisation energy indicates that the promoted electron resides in a LUMO that encompasses the alkynylene group and part of the biphenylene unit. Relative to the corresponding compound lacking the strap, it appears that electron delocalisation is somewhat more extensive in  $\text{Ru}(\text{L}_1)\text{Ru}$ . A tentative explanation for this observation is that the orientation of the biphenylene unit is more conducive for electron delocalisation.

The central cyclophane used as a constraining strap is too small to accommodate guest species but the length of the strap is easily varied by incorporating additional methylene groups. The attachment sites need not be O atoms and on-going work indicates that related structures can be formed from S atoms. These materials are especially appealing because the conformation can be switched by electrochemical approaches. It is also likely that amino groups could be used as attachment sites. One obvious drawback with this approach is that the resultant binuclear complexes possess limited solubility in organic solvents, especially at the low temperatures used for the luminescence studies. Improved solubility might be expected for those derivatives having longer straps. Such systems are currently under investigation in our laboratory.

### Acknowledgements

This work was supported by the EPSRC (GR/R23305/01). We thank the EPSRC Mass Spectrometry Facility at Swansea and Dr. Dave Parker (Durham University) for the MALDI mass spectrum measurement.

### References

1. Akiyama, M.; Watanabe, T.; Kakihana, M. *J. Phys. Chem.* **1986**, *90*, 1752.
2. Harriman, A.; Romero, F. M.; Ziessel, R.; Benniston, A. C. *J. Phys. Chem. A* **1999**, *103*, 5399.
3. (a) Feiring, A. E.; Auman, B. C.; Wonchoba, E. R. *Macromol.* **1993**, *26*, 2779; (b) Goodson, F. E.; Wallow, T. I.; Novak, B. M. *Macromol.* **1998**, *31*, 2047.
4. Analytical data for **1**:  $^1\text{H}$  NMR (300 MHz,  $\text{CDCl}_3$ )  $\delta = 2.03$  (q, 2H,  $J = 5.2 \text{ Hz}$ ,  $\text{CH}_2\text{CH}_2\text{O}$ ), 4.35 (br, 4H,  $\text{OCH}_2$ ), 6.96 (d, 2H,  $J = 7.8 \text{ Hz}$ , Ar-H<sub>6</sub>), 7.45–7.48 (m, 4H, Ar-H<sub>3,5</sub>). MS (EI)  $m/z = 478$  (calcd 477.89 for  $\text{C}_{15}\text{H}_{12}\text{I}_2\text{O}_2$ ).
5. Sonogashira, K.; Tohda, Y.; Hagihara, N. *Tetrahedron Lett.* **1975**, *16*, 4467.
6. (a) Potts, K. T.; Konwar, D. *J. Org. Chem.* **1991**, *56*, 4815; (b) Constable, E. C.; Ward, M. D. *J. Chem. Soc., Dalton Trans.* **1990**, 1405; (c) Grosshenny, V.; Romero, F. M.; Ziessel, R. *J. Org. Chem.* **1997**, *62*, 1491.
7. Analytical data for **L**<sub>1</sub>:  $^1\text{H}$  NMR (300 MHz,  $\text{CDCl}_3$ )  $\delta = 2.12$  (m, 2H,  $\text{CH}_2\text{CH}_2\text{O}$ ), 4.46 (t, 4H,  $J = 5.0 \text{ Hz}$ ,  $\text{OCH}_2$ ), 7.31–7.41 (m, 10H, py-H<sub>5,5'</sub>, Ar-H<sub>3,5,6</sub>), 7.90 (dt, 4H,  $J = 7.7 \text{ Hz}$ ,  $J' = 1.8 \text{ Hz}$ ,  $\text{terp-H}_{4,4'}$ ), 8.62 (s, 4H,  $\text{terp-H}_{3,5}$ ), 8.65 (m, 4H,  $\text{terp-H}_{3,3'}$ ), 8.75 (m, 4H,  $\text{terp-H}_{6,6'}$ ).  $^{13}\text{C}$  NMR ( $\text{CDCl}_3$ )  $\delta = 29.8$ , 71.4, 88.0, 93.6, 121.2, 121.3, 122.9, 123.0, 124.0, 126.9, 130.0, 132.7, 133.1, 136.9, 149.2, 155.6, 155.7, 157.1. MS (EI)  $m/z = 736$  (calcd 736.26 for  $\text{C}_{49}\text{H}_{32}\text{N}_6\text{O}_2$ ). CHN analysis for  $\text{C}_{49}\text{H}_{32}\text{N}_6\text{O}_2 \cdot \text{H}_2\text{O}$  calcd (found) C, 77.97 (78.00); H, 4.54 (3.81); N, 11.13 (11.07).
8. Suen, H. F.; Wilson, S. W.; Pomerantz, M.; Walsh, J. L. *Inorg. Chem.* **1989**, *28*, 786.
9. Analytical data for  $[\text{Ru}(\text{L}_1)\text{Ru}](\text{PF}_6)_4$ :  $^1\text{H}$  NMR (500 MHz,  $\text{CD}_3\text{CN}$ , 298 K)  $\delta = 2.11$  (m, 2H,  $\text{OCH}_2\text{CH}_2$ ), 4.53 (t, 4H,  $J = 5.1 \text{ Hz}$ ,  $\text{OCH}_2$ ), 7.15–7.21 (m, 8H,  $\text{terp-H}_{4,4'}$ ), 7.36–7.40 (m, 8H,  $\text{terp-H}_{3,3'}$ ), 7.51 (d, 2H,  $J = 7.6 \text{ Hz}$ , Ar-H<sub>6</sub>), 7.59 (dd, 2H,  $J = 7.6 \text{ Hz}$ ,  $J' = 1.5 \text{ Hz}$ , Ar-H<sub>5</sub>), 7.62 (d, 2H,  $J = 1.5 \text{ Hz}$ , Ar-H<sub>3</sub>), 7.91–7.97 (m, 8H,  $\text{terp-H}_{5,5'}$ ), 8.42 (t, 2H,  $J = 8.2 \text{ Hz}$ ,  $\text{terp-H}_4$ ), 8.49 (d, 4H,  $J = 7.9 \text{ Hz}$ ,  $\text{terp-H}_{6,6'}$ ), 8.52 (d, 4H,  $J = 8.0 \text{ Hz}$ ,  $\text{terp-H}_{6,6'}$ ), 8.76 (d, 4H,  $J = 8.2 \text{ Hz}$ ,  $\text{terp-H}_{3,5}$ ), 8.88 (s, 4H,  $\text{terp-H}_{3,5'}$ ). MS (MALDI)  $m/z = 1841$  (M– $\text{PF}_6$ ), CHN analysis for  $\text{C}_{79}\text{H}_{54}\text{F}_{24}\text{N}_{12}\text{O}_2\text{P}_4\text{Ru}_2 \cdot 2\text{H}_2\text{O}$  calcd (found) C, 46.94 (47.02); H, 2.89 (2.69); N, 8.32 (8.50).
10. Detailed molecular modelling calculations were carried out using the commercial package Gaussian 98, and the 6-31G basis set. Dynamic calculations were carried out to sample the potential-energy surface map from which the two conformations were identified.